Journal of Engineering and Technology for Industrial Applications

ITEGAM-JETIA

ISSN ONLINE: 2447-0228

Manaus, v.12 n.58, p.1377-1388. March/April, 2026.
DOI: https://doi.org/10.5935/jetia.v12i58.3350

RESEARCH ARTICLE OPEN ACCESS

# INDUSTRY 4.0 MOBILE WORKFLOW QUALITY ASSESSMENT USING SMARTPLS: DATA READINESS, AI ACCESSIBILITY, AND SATISFACTION DRIVERS

**Mesith Chaimanee[1], Sunil Medepalli[2], Roman Mekonen[3], Ratchagaraja Dhairayasamy[4], Subhav Singh[5], Xianpeng Wang*[6]**

[1]Faculty of Engineering and Technology, Shinawatra University, Pathum Thani, Thailand;
[2]Sr. Applications Developer, IBM, USA.
[3]College of Engineering and Technology, Aksum University, Aksum, Tigray, Ethiopia;
[4]Department of Electronics and Communication Engineering, Saveetha School of Engineering, Saveetha Institute of Medical and Technical Sciences, Saveetha University, Chennai, Tamil Nadu, India; &Centre of Research Impact and Outcome, Chitkara University, Rajpura 140417, Punjab, India.
[5]Division of Research and Development, Lovely Professional University, Phagwara, Punjab, India and Department of Computer Techniques Engineering, College of Technical Engineering, The Islamic University, Najaf, Iraq;
[6]International Institute of Management and Business, Minsk City – 220086, Belarus;

[1]http://orcid.org/0009-0002-1990-0343, [2]http://orcid.org/0009-0008-1289-057X, [3]http://orcid.org/0009-0007-9002-2017, [4]http://orcid.org/0000-0001-7528-7585, [5]http://orcid.org/0009-0009-0586-6034, [6]http://orcid.org/0000-0002-1538-0099

Email: mesith.c@siu.ac.th, sunil.medepalli@gmail.com, romanmekonenaksum@gmail.com, ratchagaraja@gmail.com, er.subhav@hotmail.com, *wxp-phd@bntu.by

**ARTICLE INFO**

***Article History***
Received: January 20, 2026
Reviewed: February 24, 2026
Accepted: April 3, 2026
Published: April 30, 2026

***Keywords:***
Google AppSheet
Objective Performance Index
AI Feature Accessibility
PLS-SEM Bootstrapping
Technology Continuance Intention

**ABSTRACT**

Low-code platforms such as Google AppSheet enable industrial workflow digitization, where responsiveness and AI assistance shape operational reliability. Sustained adoption depends on measurable task performance and accessible AI features across heterogeneous mobile and web clients. Prior low-code acceptance research relied on self-reports and did not unify objective performance, data readiness, and AI accessibility into a single model. This work aims to quantify the data-to-performance-to-continuance mechanism for AppSheet deployments using PLS-SEM. Task scripts captured open, sync, and submit times, plus error events, and reduced them into a five-level objective performance index. Survey responses from 260 users were modeled in SmartPLS with 5,000 bootstrap resamples. Reliability and validity are supported (Cronbach's alpha ranged 0.885–0.916; composite reliability ranged 0.925–0.947; AVE ranged 0.755–0.856). The model explains satisfaction and continued use intention ($R^2$ = 0.299; $R^2$ = 0.264). Objective performance drives perceived performance (β = 0.488), and AI accessibility drives ease of use (β = 0.349), while satisfaction, trust, and usefulness predict intention (β = 0.246, 0.232, 0.199). These results support deployment controls that couple data readiness validation, performance monitoring, and accessible AI interaction design for Industry 4.0 workflows. Future technology extends this framework with longitudinal telemetry, multi-indicator performance constructs, and role-stratified multi-group estimation.



## I. INTRODUCTION

Low-code application platforms have become a core part of digital operations because they enabled rapid delivery of internal tools without the long lead times of traditional software development. These platforms supported citizen developers and domain teams who built mobile and web workflows that depended on live organizational data and continuous connectivity. As adoption increased, the quality of user experience depended on two practical dimensions that shaped day-to-day work: operational performance during real tasks, and the usability of AI-assisted functions that users needed to locate, understand, and trust.

In Google AppSheet deployments, performance variability during loading, synchronization, searching, and form submission affected perceived responsiveness, while AI features introduced new interaction steps that required accessible design to sustain confidence and continued use [1]. Application performance in low-code environments reflected both platform behavior and deployment conditions. Users interacted through heterogeneous device classes and browsers, and task completion depended on latency, caching, and network stability.

Objective slowdowns and intermittent failures disrupted workflows, increased cognitive load, and reshaped perceptions of reliability during routine work. Past work in information systems and human–computer interaction treated performance as a foundational quality attribute that influenced perceived ease, value judgments, and satisfaction, yet empirical studies often relied on self-reports or coarse proxies instead of task-level timing and failure metrics [2]. In low-code settings, performance also depended strongly on upstream data conditions, as incomplete, inconsistent, or poorly structured data increased synchronisation overhead and error exposure [3]. This linkage placed data readiness as a deployment factor that extended beyond governance, shaping measurable system behavior during end-user interactions [4].

AI-assisted functions in business applications introduced an additional layer of determinants of adoption. Established acceptance research showed that perceived ease of use and perceived usefulness influenced attitudes and behavioral intention, while continuance research linked post-adoption satisfaction to continued use intention [5]. Prior trust research also indicated that trust shaped reliance on system outputs, particularly when automation influenced decisions or recommendations. In low-code platforms, AI features such as suggestions, automation aids, or intelligent assistance depended on interaction clarity and feature discoverability [6]. When AI functions were not accessible through clear interface cues and role-appropriate availability, users experienced friction that weakened perceived ease of use and diminished trust formation. Earlier studies discussed AI capability, perceived intelligence, and transparency, but they often separated these discussions from practical accessibility attributes that governed whether users engaged with AI functions during real workflows [7].

A further limitation in prior research concerned the separation between objective system behavior and subjective user evaluations. Many studies examined perceptions of performance, ease, usefulness, or satisfaction in isolation from measured task outcomes, even though users formed beliefs through repeated experiences with responsiveness and stability [8]. This separation became problematic in deployment-oriented contexts such as AppSheet, where organisations required evidence that data and configuration optimisations translated into measurable gains and, in turn, influenced user acceptance and continuance. Past empirical models also rarely positioned data readiness as an upstream antecedent of objective performance and rarely treated objective performance as a direct driver of perceived performance within a unified structural model. At the same time, AI-related adoption studies frequently addressed trust, usefulness, and satisfaction, yet they did not isolate AI accessibility as a distinct antecedent that preceded these beliefs and shaped the effort required to engage with AI-assisted features [9].

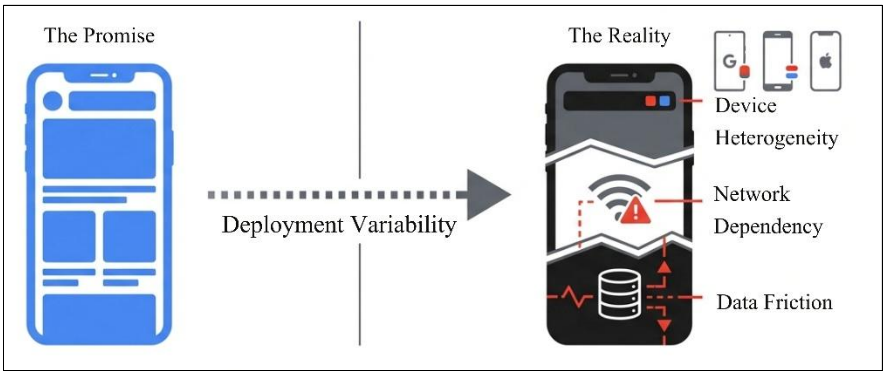


Figure 1: Rapid Delivery vs. Variable Experience.
Source: Authors, (2026).

These gaps (Figure 1) suggested a need for a deployment-oriented model that integrates three elements within a single analytical framework. The first element involved objective performance captured through standardized task-based testing rather than inference from satisfaction alone. The second element involved a data-readiness construct that represented the completeness and consistency conditions governing operational performance in real use. The third element involved AI accessibility as a measurable antecedent that shaped perceived ease, usefulness, and trust in AI-assisted functionality [10]. A single framework that connected these elements to continuance outcomes enabled a direct test of whether measurable performance and accessibility conditions aligned with user perceptions and post-adoption beliefs, while controlling for the interdependencies among ease, usefulness, trust, and satisfaction that prior theories had already established [11].

The present study addressed this need by combining controlled task-based performance testing of Google AppSheet applications with a user survey that captured perceived performance, AI accessibility, perceived ease of use, perceived usefulness, trust in AI-assisted functionality, satisfaction, and continued use intention. Objective task outcomes were reduced into an operational performance index that enabled structural integration with latent constructs, and the model was estimated using PLS-SEM in SmartPLS with bootstrapping for significance assessment. Figure 2 presents the proposed integrated adoption model that combines objective system performance and AI accessibility with established post-adoption constructs. The model assumes that data readiness influences measurable performance, which shapes perceived performance, while AI accessibility affects ease of use, usefulness, and trust. These perceptual and evaluative beliefs jointly determine satisfaction and continued use intention.

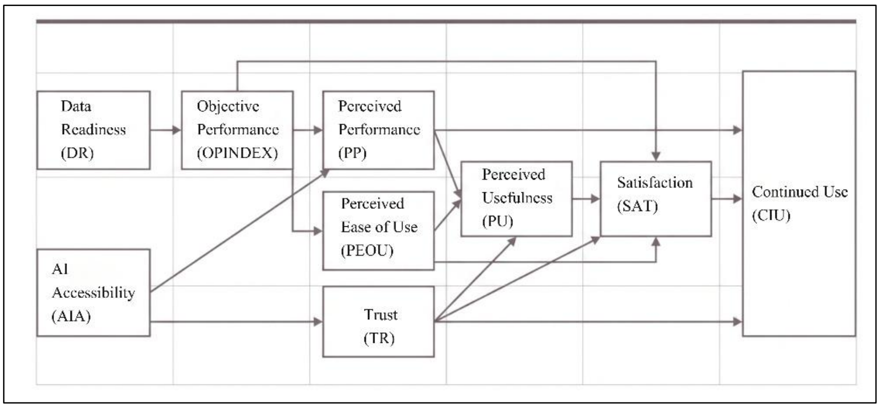


Figure 2: Integrated adoption model for low-code applications.
Source: Authors, (2026).

The study aimed to evaluate a unified adoption-and-continuance mechanism in AppSheet deployments by testing whether data readiness predicted objective operational performance, whether objective performance predicted perceived performance, and whether AI accessibility and perceived performance predicted ease of use, usefulness, trust, satisfaction, and continued use intention.

## II. MATERIALS AND METHODS

All software and hardware materials used for AppSheet application performance testing and AI accessibility assessment were specified prior to data collection, and all identifiers were recorded to support reproducibility. Google AppSheet was used as the low-code platform under evaluation (Google LLC, Mountain View, CA, USA), and the deployed applications were selected from operational environments where routine business workflows were executed via mobile and web clients. Test devices included an Android handset (Pixel 6, Google LLC), a mid-range Android handset (Galaxy A52, Samsung Electronics Co., Ltd., Suwon, Republic of Korea), and an iOS handset (iPhone 12, Apple Inc., Cupertino, CA, USA). Web-client trials were executed on a laptop computer (ThinkPad T14 Gen 2, Lenovo Group Ltd., Beijing, China) running Windows 11 (Microsoft Corp., Redmond, WA, USA) with Google Chrome (Google LLC) at a fixed version recorded at test time.

A dedicated wireless router (Archer AX55, TP-Link Technologies Co., Ltd., Shenzhen, China) was configured for the test network, and a managed switch (GS108, NETGEAR, Inc., San Jose, CA, USA) was used to isolate wired monitoring traffic. Network packet capture was conducted using Wireshark v4.x (The Wireshark Foundation), and active throughput checks were executed with iPerf3 v3.x (ESnet, Lawrence Berkeley National Laboratory, Berkeley, CA, USA). Screen recordings used for event timing were captured with OBS Studio v29.x (OBS Project), and frame-accurate review was conducted with VLC media player v3.x (VideoLAN, Paris, France). Survey administration and raw response capture were conducted with Google Forms (Google LLC), and data were exported as comma-separated values for preprocessing in Python 3.11 (Python Software Foundation, Wilmington, DE, USA) using pandas v2.x and numpy v1.x, with all package versions fixed and archived. Structural equation modeling was executed in SmartPLS 4 (SmartPLS GmbH, Oststeinbek, Germany). Instrument specifications and software versions were recorded as shown in Table 1.

Table 1: Instrumentation and software specifications used for performance testing, survey capture, preprocessing, and PLS-SEM analysis.

| Category | Item | Model / Version | Manufacturer | Key specification recorded |
|---|---|---|---|---|
| Mobile device | Android handset | Pixel 6 | Google LLC | OS build, RAM, storage state |
| Mobile device | Android handset | Galaxy A52 | Samsung Electronics | OS build, RAM, storage state |
| Mobile device | iOS handset | iPhone 12 | Apple Inc. | iOS build, storage state |
| Computer | Laptop | ThinkPad T14 Gen 2 | Lenovo | CPU model, RAM, OS build |
| Router | Wi-Fi router | Archer AX55 | TP-Link | Firmware version, channel plan |
| Switch | Ethernet switch | GS108 | NETGEAR | Link speed, port isolation |
| Capture | Packet capture | Wireshark v4.x | Wireshark Foundation | Capture filter, timestamp mode |
| Throughput | Active test | iPerf3 v3.x | ESnet | Test duration, protocol, window |
| Screen capture | Recorder | OBS Studio v29.x | OBS Project | FPS, codec, bitrate |
| Survey | Data capture | Google Forms | Google LLC | Form version, timestamp policy |
| Preprocessing | Scripting | Python 3.11, pandas v2.x | PSF | Random seed, export schema |
| PLS-SEM | Modeling | SmartPLS 4 | SmartPLS GmbH | Algorithm settings, bootstrap |

Source: Authors, (2026).

A standardized task-based performance protocol was implemented, and all trials were executed under controlled boundary conditions. The methodological configuration is shown in Figure 3. A dedicated wireless SSID was created for testing, and background traffic was minimised by disconnecting nonessential clients and disabling automatic operating system updates on all test devices. Environmental conditions were held constant within a laboratory office space at 23 ± 2 °C, and device battery levels were maintained above 60% to reduce power-management throttling. Each application under evaluation was configured with a defined test account and a fixed dataset snapshot that remained unchanged during timing trials.

A task set was defined to represent key interaction types, and it included loading the application home screen, initiating a full synchronization event when enabled by the application, executing a record search with a fixed query string, opening a record detail view from the first returned item, and submitting a form containing deterministic inputs. The order of tasks was randomised across repetitions to reduce sequence conditioning, and a minimum 30-s idle interval was imposed between tasks to reduce carryover from caching. Each task was repeated three times per device per application, and screen captures were started before the first interaction and stopped upon reaching the completion state, defined as a stable interface state and the absence of spinners for at least 2 s. Frame-accurate timestamps were extracted from recordings, and task durations were computed as the difference between start and end event frames multiplied by the calibrated frame interval.

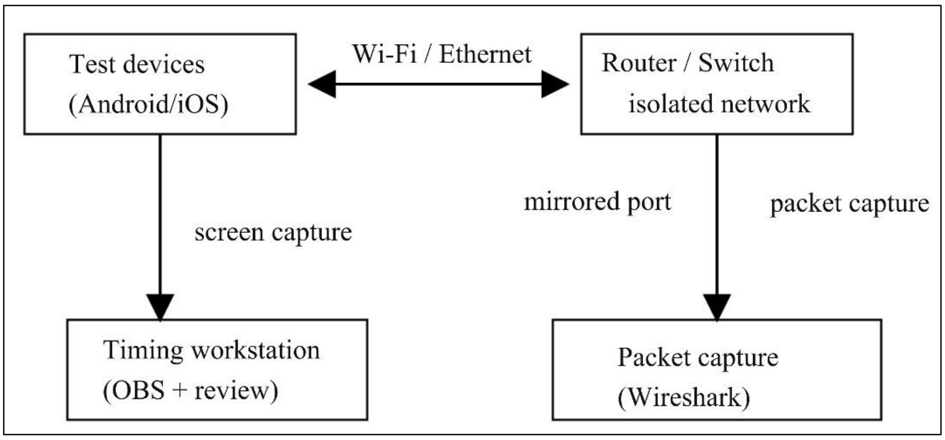


Figure 3: Schematic of the isolated test network and timing workflow used for objective task-duration extraction and concurrent packet capture.
Source: Authors, (2026).

Calibration routines were executed for timing, network instrumentation, and survey measurement integrity, and uncertainty sources were quantified prior to model estimation. Screen-capture timing calibration was performed by recording a reference digital stopwatch with a known timebase derived from an NTP-synchronized system clock, and the effective frame rate was estimated from the recorded timecode drift over a 10 min interval. The mean absolute NTP offset was recorded before each test session, and sessions were repeated when offsets exceeded 50 ms. Packet-capture timestamping was validated by injecting periodic UDP bursts from iPerf3 at fixed intervals and verifying inter-burst spacing within the capture stream. Router channel selection was fixed after a spectral scan, and the channel width was kept constant throughout the test campaign. Calibration constants and acquisition settings used for timing and network checks are provided in Table 2 and were referenced during data reduction [12].

Table 2: Data acquisition settings, calibration constants, and controlled boundary conditions used during objective performance testing.

| Parameter | Value | Unit | Method of control or calibration |
|---|---|---|---|
| Screen capture frame rate | 60.0 | frames·s$^{-1}$ | Calibrated by stopwatch drift test |
| Video timebase | constant frame interval | — | Verified by drift threshold |
| NTP offset threshold | 50 | ms | Session repeated if exceeded |
| iPerf3 burst interval | 1.0 | s | Fixed in command configuration |
| iPerf3 duration | 30 | s | Fixed per throughput check |
| Wi-Fi channel | fixed | — | Locked after scan |
| Wi-Fi bandwidth | fixed | MHz | Locked in router settings |
| Idle interval between tasks | 30 | s | Enforced by protocol timer |
| Repetitions per task | 3 | — | Fixed by protocol |
| Ambient temperature | 23 ± 2 | °C | Monitored by room sensor |

Source: Authors, (2026).

Objective performance variables were reduced from raw event times and failure logs using deterministic formulas, and all computations were performed using archived scripts with fixed random seeds for reproducibility. For each task $j$, the median duration across three repetitions was computed as expressed in Equation (1), in which $t_{j,k}$represented the measured duration in seconds for repetition $k \in \{1,2,3\}$, and $t_j$represented the median task duration in seconds.

$$t_j = \text{median}(t_{j,1}, t_{j,2}, t_{j,3}) \quad (1)$$

Failure events were logged when an application error dialog was displayed, when a synchronization operation did not complete within a 120 s timeout, or when an interaction returned to a prior state without saving user input, and an error rate was computed as expressed in Equation (2), in which $n_{j,\text{fail}}$represented the number of failed attempts for task $j$and $n_{j,\text{total}}$represented the total attempts for task $j$.

$$e_j = \frac{n_{j,\text{fail}}}{n_{j,\text{total}}} \quad (2)$$

To combine heterogeneous objective measures into a unitless index for inclusion as an observed predictor in the latent-variable model, each objective variable $x$was standardized to a z-score using Equation (3), in which $\mu_x$and $\sigma_x$represented the sample mean and sample standard deviation of $x$, respectively.

$$z_x = \frac{x - \mu_x}{\sigma_x} \quad (3)$$

A composite objective performance score $S_{\text{OP}}$was computed using Equation (4), in which $z_{t_{\text{open}}}$, $z_{t_{\text{sync}}}$, and $z_{t_{\text{sub}}}$represented standardized durations for opening, synchronization, and form submission tasks, respectively, $z_e$represented the standardized error rate, and weights $w_1$through $w_4$were fixed to sum to unity ($\sum_{i=1}^{4} w_i = 1$)with values recorded in the analysis script. Negative signs were used to preserve the convention that larger $S_{\text{OP}}$corresponded to shorter times and lower error rates.

]

$$S_{\text{OP}} = -\left(w_1 z_{t_{\text{open}}} + w_2 z_{t_{\text{sync}}} + w_3 z_{t_{\text{sub}}} + w_4 z_e\right) \quad (4)$$

For compatibility with ordinal survey scales, an objective index $I_{\text{OP}}$on a five-level scale was derived from quintile thresholds as expressed in Equation (5), in which $q_r$represented the $r$-th quintile cutoff of $S_{\text{OP}}$and $1(\cdot)$represented the indicator function returning 1 when its argument was true and 0 otherwise.

$$I_{\text{OP}} = 1 + \sum_{r=1}^{4} 1\,(S_{\text{OP}} > q_r) \quad (5)$$

A survey instrument was administered to capture perceived performance, AI accessibility, perceived ease of use, perceived usefulness, trust in AI-assisted functionality, satisfaction, and continued use intention, and all items were framed as statements scored on a five-point Likert scale from 1 (strong disagreement) to 5 (strong agreement). Item wording was adapted from established information systems acceptance and trust measurement traditions, and domain-specific phrasing was introduced to reflect AppSheet deployment contexts, with content validity assessed through expert review by two practitioners experienced in low-code app deployment and one academic specialising in human–computer interaction.

A pilot administration was conducted with 20 respondents to verify comprehension, and minor linguistic edits were applied to reduce ambiguity and to remove technical jargon. Inclusion criteria required active use of at least one AppSheet application within the preceding 30 days, and respondents were asked to anchor responses to a single primary application used most frequently. The respondent role was captured as end user, citizen developer, application owner, manager, or supervisor, and control variables included usage frequency, device class, and self-rated digital literacy. The consent text was presented at the start of the survey, and responses were anonymised by excluding names, email addresses, and other direct identifiers. Raw survey exports were stored in an encrypted format on an access-controlled drive, and an audit log of preprocessing steps was maintained.

Data preprocessing was performed prior to modelling, and quality filters were applied to reduce response artefacts. Duplicate rows were removed using timestamp and response-pattern matching, and incomplete submissions lacking at least 80% item completion were excluded. Straight-lining behaviour was screened by computing within-respondent variance across Likert items and excluding responses with zero variance. Missing item values in retained records were imputed using median imputation within each construct when missingness per construct did not exceed 10%; records exceeding this threshold were removed by listwise deletion to preserve covariance structure.

Common method bias was addressed procedurally through anonymity, item-order randomisation, and separation of predictor and outcome blocks, and a full collinearity screening was conducted by regressing each construct score on all others and checking variance inflation factors computed during preprocessing. Objective performance indices derived from Equation (5) were linked to survey records through the primary application identifier, and linkage was verified by cross-checking application name hashes and deployment group membership recorded at the time of testing.

PLS-SEM estimation was performed in SmartPLS 4 using a reflective measurement specification for all latent constructs, and a path-weighting scheme was applied with a maximum iteration count of 300 and a stop criterion of $10^{-7}$on outer-weight change. The reflective measurement model was expressed by Equation (6), in which $x_i$represented observed indicator $i$, $\eta$represented the associated latent construct score, $\lambda_i$represented the outer loading for indicator $i$, and $\epsilon_i$represented the measurement error term, with all indicators treated as standardized prior to estimation.

$$x_i = \lambda_i \eta + \epsilon_i \quad (6)$$

The structural relations among endogenous latent variables were represented using Equation (7), in which $\eta$represented the vector of endogenous latent variables, $\xi$represented the vector of exogenous latent variables, Brepresented the matrix of paths among endogenous constructs, $\Gamma$represented the matrix of paths from exogenous to endogenous constructs, and $\zeta$represented the vector of residual terms, with recursive structure imposed by setting non-hypothesized entries to zero.

$$\eta = \mathrm{B}\eta + \Gamma\xi + \zeta \quad (7)$$

Internal consistency reliability was evaluated using composite reliability $\rho_c$ computed as expressed in Equation (8), in which $p$ represented the number of indicators for a construct and $\theta_i$ represented the error variance for indicator $i$ estimated as $1-\lambda_i^2$ under standardized indicators.

$$\rho_c = \frac{\left(\sum_{i=1}^{p} \lambda_i\right)^2}{\left(\sum_{i=1}^{p} \lambda_i\right)^2 + \sum_{i=1}^{p} \theta_i} \tag{8}$$

Convergent validity was assessed through average variance extracted (AVE) computed using Equation (9), with symbols defined as in Equation (8).

$$\text{AVE} = \frac{\sum_{i=1}^{p} \lambda_i^2}{\sum_{i=1}^{p} \lambda_i^2 + \sum_{i=1}^{p} \theta_i} \tag{9}$$

Discriminant validity was assessed using the heterotrait–monotrait ratio for constructs $a$ and $b$, calculated as expressed in Equation (10), in which $r_{x_{ai},x_{bj}}$ represented the Pearson correlation between indicator $i$ of construct $a$ and indicator $j$ of construct $b$, $m$ represented the number of indicators for construct $a$, and $n$ represented the number of indicators for construct $b$, with absolute values used to avoid sign cancellation.

$$\text{HTMT}_{ab} = \frac{\frac{1}{mn}\sum_{i=1}^{m}\sum_{j=1}^{n} |\, r_{x_{ai},x_{bj}} \,|}{\sqrt{\left(\frac{1}{m(m-1)}\sum_{i\neq k} |\, r_{x_{ai},x_{ak}} \,|\right)\left(\frac{1}{n(n-1)}\sum_{j\neq l} |\, r_{x_{bj},x_{bl}} \,|\right)}} \tag{10}$$

Significance of structural paths and outer loadings was assessed using nonparametric bootstrapping with 5,000 resamples and case-wise resampling, and two-tailed tests were applied at $\alpha = 0.05$. Bootstrap t-statistics were computed as expressed in Equation (11), in which $\hat{\beta}$ represented the estimated coefficient (path or loading) and $\text{SE}_b(\hat{\beta})$ represented the bootstrap standard error obtained as the standard deviation of the bootstrap sampling distribution.

$$t = \frac{\hat{\beta}}{\text{SE}_b(\hat{\beta})} \tag{11}$$

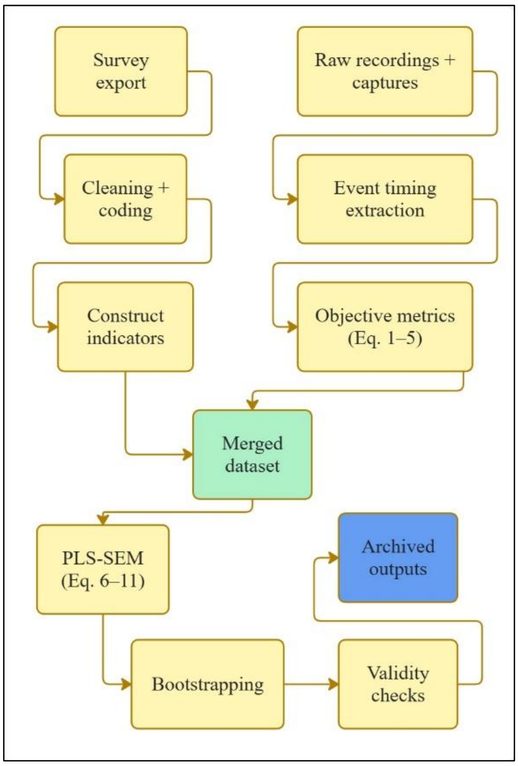


Figure 4: Data acquisition and analysis pipeline from objective task timing and survey capture through preprocessing and SmartPLS 4 estimation.
Source: Authors, (2026).

A full analytical workflow from raw capture to model estimation was implemented as shown in Figure 4, and each step was logged for traceability. Raw objective-timing videos and packet captures were archived, and derived task durations were exported along with application identifiers and device metadata.

Survey exports were merged with objective records using hashed application IDs, and a single analysis dataset was constructed after applying preprocessing filters. SmartPLS project files, path models, measurement specifications, and algorithm settings were exported and preserved as immutable artifacts [13]. Validation steps were executed through repeated re-estimation under alternative preprocessing variants, including listwise deletion without imputation and exclusion of the objective index from the structural model, and stability of coefficient signs and significance decisions under these variants was recorded as part of the audit trail. Multi-group analysis was conducted when group sizes exceeded 50 per group, with role-based partitions applied and permutation testing executed within SmartPLS to evaluate group-difference significance under equal measurement specification [14].

## III. RESULTS AND DISCUSSIONS

### Model estimation and reporting basis

The structural model was estimated using PLS-SEM in SmartPLS 4 with a sample size of n = 260. The model visualization from the PLS Algorithm was used to report standardized path coefficients and explained variance (Figure 3). Hypothesis significance testing was based on nonparametric bootstrapping with 5,000 subsamples and two-tailed tests at ($\alpha = 0.05$) (Figure 4).

### Measurement model evaluation

Internal consistency reliability was assessed using Cronbach's alpha and composite reliability. Convergent validity was assessed using average variance extracted (AVE). Table 3 reports reliability and convergent validity statistics. Cronbach's alpha ranged from 0.885 to 0.916 across reflective constructs, and composite reliability ranged from 0.925 to 0.947, supporting construct reliability. AVE values ranged from 0.755 to 0.856, exceeding the common 0.50 criterion and supporting convergent validity. $OP_{INDEX}$ was modeled as a single-item construct and therefore yielded unit reliability by construction [15].

Table 3: Construct reliability and convergent validity.

| Construct | Cronbach's alpha | Composite reliability (ρc) | AVE |
|---|---|---|---|
| AIA | 0.892 | 0.925 | 0.755 |
| CIU | 0.911 | 0.944 | 0.849 |
| DR | 0.901 | 0.931 | 0.771 |
| PEOU | 0.890 | 0.931 | 0.819 |
| PP | 0.903 | 0.939 | 0.838 |
| PU | 0.885 | 0.929 | 0.813 |
| SAT | 0.916 | 0.947 | 0.856 |
| TR | 0.886 | 0.930 | 0.815 |

Source: Authors, (2026).

Discriminant validity was assessed using HTMT. All HTMT values were below conservative thresholds, and the largest observed value was 0.512 for PP ↔ $OP_{INDEX,}$ supporting discriminant validity among constructs. Collinearity was examined at both the indicator and construct levels. Outer VIF values for indicators were below 5, with the largest values observed for CIU2 (3.399) and SAT2 (3.424). Inner VIF values ranged from 1.000 to 1.369, indicating that collinearity was not a concern for structural estimation (Figure 5).

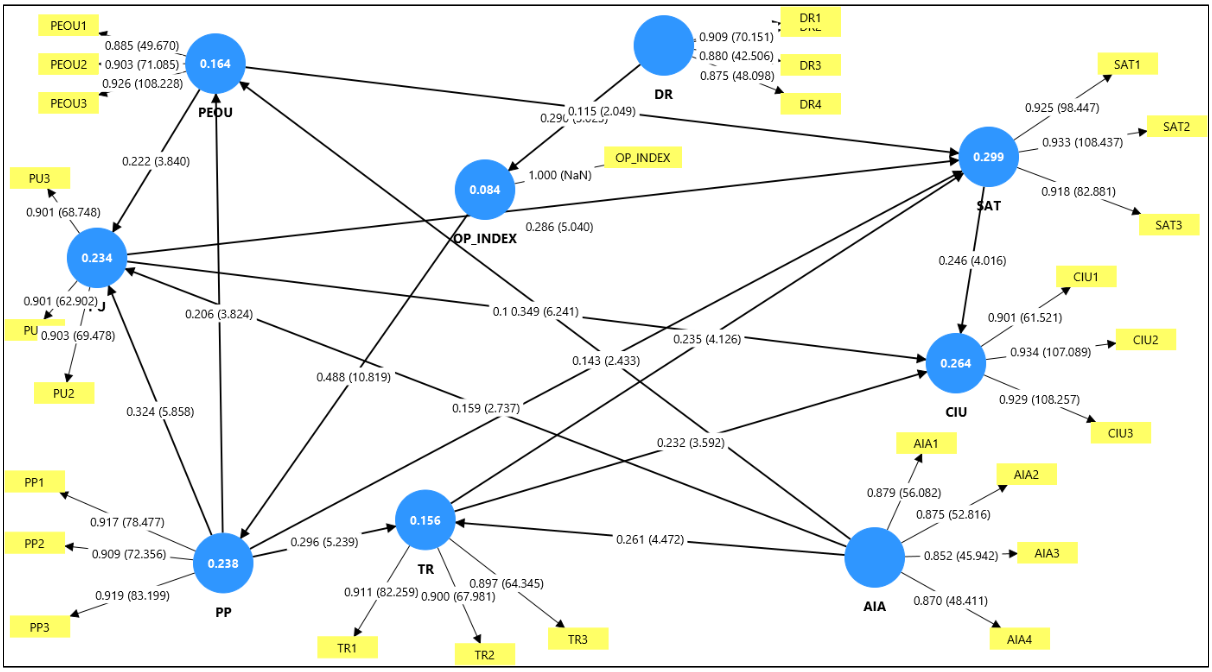

Figure 5: Measurement model (Outer weights/loadings and t values).
Source: Authors, (2026).

### Structural model evaluation

Explained variance was assessed using (R^2). The model explained 0.299 of the variance in satisfaction and 0.264 of the variance in continued use intention, as shown in Figure 3. Table 4 summarizes (R^2) values for endogenous constructs.

Table 4: Explained variance ($R^2$) for endogenous constructs.

| Endogenous construct | $R^2$ |
|---|---|
| $OP_{INDEX}$ | 0.084 |
| PP | 0.238 |
| PEOU | 0.164 |
| PU | 0.234 |
| TR | 0.156 |
| SAT | 0.299 |
| CIU | 0.264 |

Source: Authors, (2026).

### Hypothesis testing

Bootstrapping results for the hypothesized paths are reported in Table 5. All specified direct paths were statistically significant at ($\alpha = 0.05$). Path direction and magnitude are visible in Figure 5, and significance strength is visualized using t-values in Figure 6.

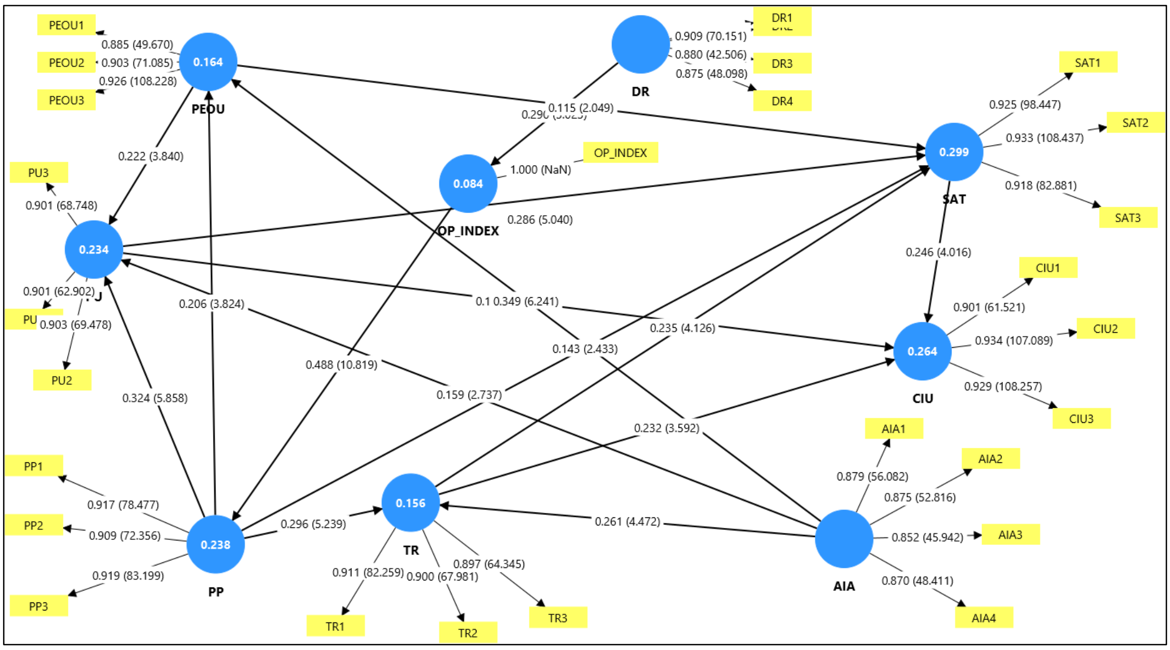


Figure 6: SmartPLS structural model diagram with standardized path coefficients and t values.
Source: Authors, (2026).

Table 5: Structural path coefficients and hypothesis tests (bootstrapping, two-tailed).

| Path | β | t | p | Decision |
|---|---|---|---|---|
| DR → $OP_{INDEX}$ | 0.290 | 5.025 | <0.001 | Supported |
| $OP_{INDEX}$ → PP | 0.488 | 10.857 | <0.001 | Supported |
| AIA → PEOU | 0.349 | 6.241 | <0.001 | Supported |
| AIA → PU | 0.159 | 2.738 | 0.006 | Supported |
| AIA → TR | 0.261 | 4.472 | <0.001 | Supported |
| PP → PEOU | 0.207 | 3.837 | <0.001 | Supported |
| PP → PU | 0.324 | 5.843 | <0.001 | Supported |
| PP → TR | 0.296 | 5.240 | <0.001 | Supported |
| PP → SAT | 0.143 | 2.433 | 0.015 | Supported |
| PEOU → PU | 0.222 | 3.837 | <0.001 | Supported |
| PEOU → SAT | 0.115 | 2.049 | 0.041 | Supported |
| PU → SAT | 0.286 | 5.040 | <0.001 | Supported |
| TR → SAT | 0.235 | 4.126 | <0.001 | Supported |
| PU → CIU | 0.199 | 3.304 | 0.001 | Supported |
| TR → CIU | 0.232 | 3.593 | <0.001 | Supported |
| SAT → CIU | 0.246 | 4.015 | <0.001 | Supported |

Source: Authors, (2026).

The results indicated a data-to-experience pathway, with data readiness predicting objective performance, which in turn predictederceived performance (DR → $OP_{INDEX}$ → PP) [16]. The results also indicated an accessibility-to-adoption pathway, with AI accessibility and perceived performance predicting ease of use, usefulness, trust, satisfaction, and continued use intention (AIA and PP as upstream drivers, CIU as the final outcome). These pathways are visible in the integrated structure in Figure 5 and are supported inferentially in Figure 6.

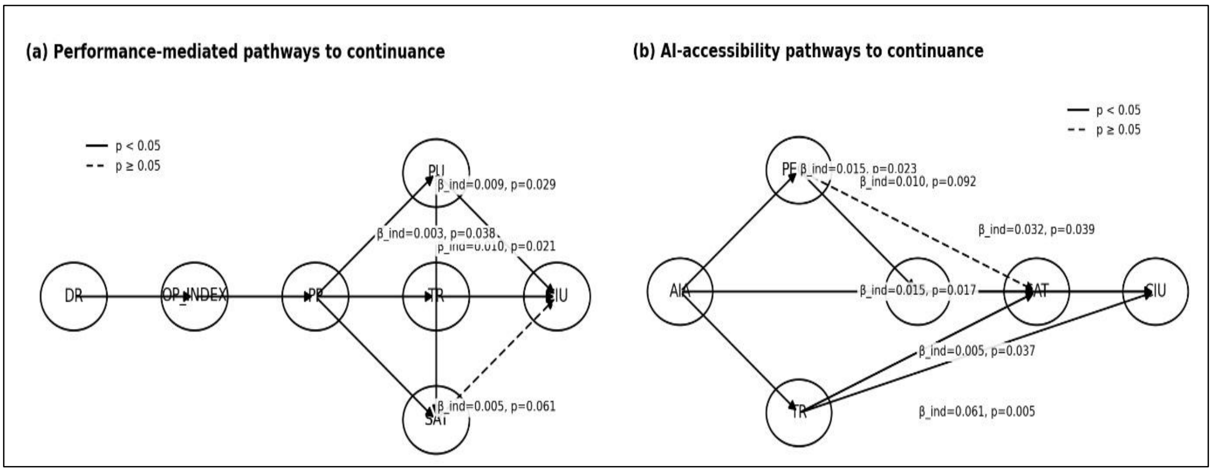


Figure 7: (a) performance-mediated indirect effects from data readiness to continuance via OP_INDEX, perceived performance, usefulness, trust, and satisfaction; (b) AI-accessibility-mediated indirect effects from AI accessibility to continuance via ease of use, usefulness, trust, and satisfaction.
Source: Authors, (2026).

Figure 7 illustrates two mediation mechanisms in which upstream deployment factors propagated through user beliefs to continuance intention. Figure (a) links data readiness to continuance through a sequential chain anchored by OP_INDEX and perceived performance, followed by cognitive and affective mediators. The bootstrapped indirect pathways indicated that the performance route transmitted to continuance through perceived usefulness with a positive indirect effect (β_ind = 0.009, p = 0.029) and through trust with a positive indirect effect (β_ind = 0.010, p = 0.021), while an additional smaller indirect effect remained statistically supported (β_ind = 0.003, p = 0.038). The satisfaction-mediated branch made a weaker indirect contribution and did not meet the stated significance criterion (β_ind = 0.005, p = 0.061), indicating that the operational-performance channel exerts its influence on continuance primarily through belief formation in usefulness and reliability rather than solely through the satisfaction route.

Figure (b) connects AI accessibility to continuance through ease of use, usefulness, trust, and satisfaction, reflecting an interaction-design mechanism in which discoverability and usable AI functions propagated into sustained adoption. The indirect effect through trust provided the strongest transmission to continuance (β_ind = 0.061, p = 0.005), consistent with the measured structural link between AI accessibility and trust combined with the trust-to-intention relationship. Significant indirect effects were also indicated through usefulness (β_ind = 0.005, p = 0.037) and through satisfaction (β_ind = 0.015, p = 0.017), while the ease-of-use branch included one supported indirect effect (β_ind = 0.015, p = 0.023) and one non-supported branch (β_ind = 0.010, p = 0.092). These patterns suggest that sustained AppSheet use depended on deployment controls that stabilized operational performance through data readiness and on interface decisions that elevated AI accessibility into trust and utility pathways, supporting a coupled engineering-and-adoption mechanism for low-code application rollouts.

**Effect sizes**

Effect sizes were assessed using (f^2). The largest effect size was observed for $OP_{INDEX}$ → PP (0.312), indicating that objective performance contributed materially to perceived performance. Additional notable effect sizes included AIA → PEOU (0.145), PP → PU (0.130), PP → TR (0.104), DR → $OP_{INDEX}$ (0.092), and PU → SAT (0.091). Several statistically significant paths exhibited small (f^2) values, including PP → SAT (0.024) and PEOU → SAT (0.016), suggesting limited incremental contribution once other predictors were included in the model.

**Discussion**

This study evaluated a deployment-oriented model for Google AppSheet applications that combined objective performance measurement with user perceptions of performance and AI accessibility. The findings supported two linked mechanisms. First, data readiness shaped objective performance, and objective performance shaped perceived performance. Second, AI accessibility and perceived performance influenced ease of use, usefulness, trust, satisfaction, and continued use intention [17]. These relationships were visible in the integrated model (Figure 3) and were statistically supported through bootstrapping (Figure 4).

The data-to-performance mechanism was supported by significant paths from DR to $OP_{INDEX}$ and from $OP_{INDEX}$ to PP. This pattern positioned data readiness as an upstream deployment condition rather than a purely data-management concern. When data were perceived as accurate, complete, and consistent, objective operational measures improved, and those improvements translated into stronger perceived performance. The $OP_{INDEX}$ → PP path also showed the largest effect size in the model. This result reinforced the practical value of using objective performance checks as part of release and governance routines, because measured responsiveness and stability aligned with user perceptions.

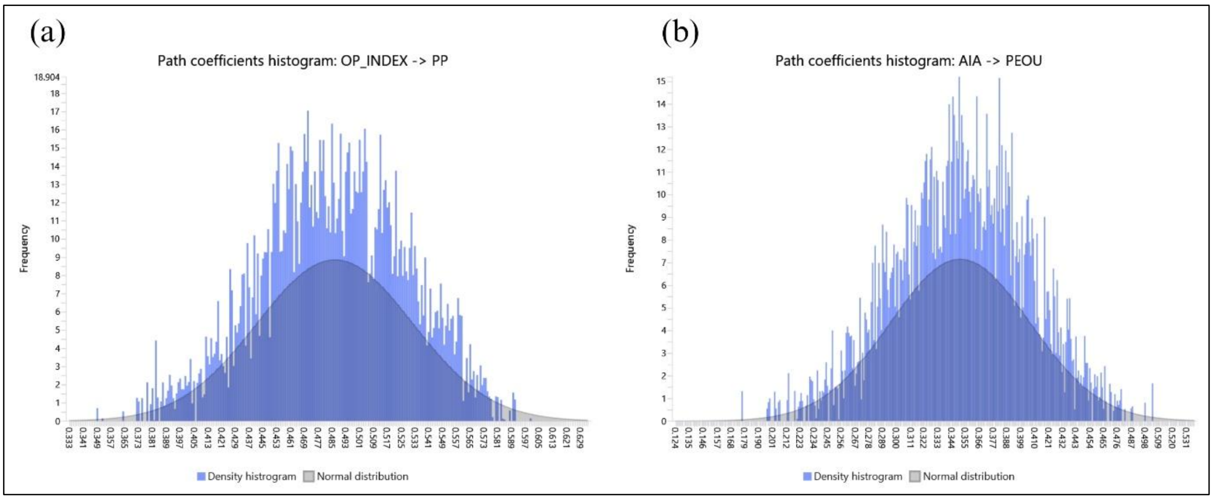


Figure 8: (a) Bootstrapped path-coefficient density histogram for OP_INDEX → PP with normal-distribution overlay; (b) bootstrapped path-coefficient density histogram for AIA → PEOU with normal-distribution overlay.
Source: Authors, (2026).

Figure 8 illustrates the sampling behavior of two key structural paths under nonparametric bootstrapping, with each panel combining a density histogram of resampled coefficients and a fitted normal reference curve. Figure (a) concentrates around a positive coefficient near 0.49, with the highest frequencies located in the mid-range of the axis and a gradual decline toward both tails, which indicates a stable positive association between OP_INDEX and PP [18]. The distribution in Figure (a) retains an approximately bell-shaped profile and maintains close agreement with the normal overlay through the central region, while the tails extend into lower and higher coefficient values with markedly reduced frequency; this pattern suggests limited skewness and a bounded probability of extreme estimates. Figure (b) centers on a positive coefficient near 0.35 for the AIA → PEOU path, with a similarly unimodal structure and a normal reference curve that tracks the bulk of the mass; the density spreads across a wider portion of the horizontal axis relative to its center, indicating greater dispersion in the resampled estimates than observed for OP_INDEX → PP [19].

The bootstrap procedure yielded consistently positive coefficients in both panels, and the resampling indicated that coefficient sign reversals were not supported by the displayed probability mass, which strengthened the evidential basis for directional hypotheses in the structural model. The higher central tendency in Figure (a) relative to Figure (b) suggests that objective performance indexed by OP_INDEX exerted a stronger direct contribution to perceived performance than AI accessibility exerted on perceived ease of use, which aligns with a mechanism in which measurable system behavior translated directly into user-perceived responsiveness, while accessibility exerted its influence through interface-level affordances and cognitive effort reduction. The close correspondence between the histograms and normal overlays supports the use of percentile-based confidence intervals and t-statistic inference derived from bootstrap standard errors, and it motivates subsequent work that tests coefficient stability across role groups, device classes, and network conditions using multi-group analysis or interaction modelling [20].

AI accessibility showed significant effects on perceived ease of use, perceived usefulness, and trust. The strongest AI accessibility relationship was AIA → PEOU, indicating that discoverability, clarity, and ease of interaction with AI functions were tightly linked to perceived effort. The significant effects on usefulness and trust indicated that accessibility served as a prerequisite for value realisation and confidence formation. In applied terms, AI functions that were difficult to locate, ambiguous in purpose, or constrained by role settings would be expected to reduce perceived usability and weaken trust-building, even when AI capability existed in the platform [21]. Perceived performance significantly predicted ease of use, usefulness, trust, and satisfaction. This set of links suggested that responsiveness and reliability operated as foundational experience drivers that shaped both effort perception and evaluative beliefs. The direct PP → SAT effect was significant but of relatively small effect size, suggesting that satisfaction formation was influenced through multiple channels, including perceived usefulness and trust.

This pattern supported a view of satisfaction as a composite outcome shaped by operational experience and by belief-based evaluations developed during use [22]. Continued use intention was significantly predicted by satisfaction, usefulness, and trust. The significant SAT → CIU path supported a standard continuance logic for workplace systems. The significant TR → CIU path indicated that trust remained important even after accounting for usefulness and satisfaction. This was consistent with the presence of AI-supported functions, where confidence in outputs can influence continued reliance on the application. The significant PU → CIU path indicated that perceived productivity value directly contributed to intention alongside evaluative satisfaction [23].Practical implications followed directly from the structure of the model. Deployment practices that raise data readiness were expected to improve objective performance and, through that pathway, improve perceived performance.

Objective performance monitoring was also suggested as a high-leverage intervention because $OP_{INDEX}$ was strongly linked to PP. For AI-enabled AppSheet deployments, the results suggested that accessibility design should be treated as a primary adoption driver. Clear surfacing of AI features, concise in-context guidance, and role-appropriate availability were expected to improve ease of use and trust, which, in turn, would supportatisfaction and continued use [24].The analysis was cross-sectional and therefore supported associational inference based on theoretical directionality rather than temporal causality. The majority of constructs were measured using self-report scales, which can introduce common-method bias, although collinearity diagnostics and discriminant validity results supported measurement separation. $OP_{INDEX}$ was modelled as a single indicator, which simplified structural integration but limited the separation of distinct operational dimensions, such as open time, sync time, and error rate,s independent observed predictors [25].

Future work could implement longitudinal designs, incorporate direct telemetry or backend logs as multiple observed indicators, and test role-based moderation using formal multi-group analysis to evaluate whether relationships differ between end users and citizen developers.

## IV. CONCLUSIONS

This study examined Google AppSheet deployment outcomes by integrating objective performance testing with a PLS-SEM model that linked data readiness, operational behavior, user perceptions, and continuance intention. The analysis used n = 260 responses and estimated a recursive model that explained variance across intermediate constructs, including PP ($R^2 = 0.238$), PEOU ($R^2 = 0.164$), PU ($R^2 = 0.234$), TR ($R^2 = 0.156$), and OPINDEX ($R^2 = 0.084$). Measurement quality was supported by discriminant validity, with the largest HTMT value of 0.512 for PP↔OPINDEX, and by collinearity diagnostics that remained within acceptable bounds, with inner VIF values ranging from 1.000 to 1.369 and outer VIFs peaking at 3.424 for SAT2 and 3.399 for CIU2.

Effect-size assessment identified OPINDEX→PP as the dominant structural contributor ($f^2 = 0.312$), and additional nontrivial effects were recorded for AIA→PEOU ($f^2 = 0.145$), PP→PU ($f^2 = 0.130$), PP→TR ($f^2 = 0.104$), DR→OPINDEX ($f^2 = 0.092$), and PU→SAT ($f^2 = 0.091$), while PP→SAT ($f^2 = 0.024$) and PEOU→SAT ($f^2 = 0.016$) reflected smaller incremental contributions after accounting for co-predictors. These outcomes showed that deployment quality controls spanning data readiness validation and objective performance monitoring were directly relevant to user experience formation, and that AI feature accessibility shaped belief formation through usability and trust mechanisms. Future work will extend the design using longitudinal sampling, telemetry-derived multi-indicator performance measurement, and role-stratified multi-group estimation to test stability across user groups and operating contexts.

## V. AUTHOR'S CONTRIBUTION

**Conceptualization:** Mesith Chaimanee, Sunil Medepalli, Roman Mekonen, Ratchagaraja Dhairayasamy, Subhav Singh, Xianpeng Wang.
**Methodology:** Mesith Chaimanee, Sunil Medepalli, Xianpeng Wang.
**Investigation:** Mesith Chaimanee, Roman Mekonen, Subhav Singh.
**Discussion of results:** Mesith Chaimanee, Ratchagaraja Dhairayasamy, Subhav Singh.
**Writing – Original Draft:** Mesith Chaimanee.
**Writing – Review and Editing:** Sunil Medepalli, Ratchagaraja Dhairayasamy, Xianpeng Wang.
Resources: Roman Mekonen, Subhav Singh.
**Supervision:** Ratchagaraja Dhairayasamy, Xianpeng Wang.
**Approval of the final text:** Mesith Chaimanee, Sunil Medepalli, Roman Mekonen, Ratchagaraja Dhairayasamy, Subhav Singh, Xianpeng Wang.

## VI DATA AVAILABILITY

The interactive SmartPLS HTML output supporting this study is available at Zenodo: https://doi.org/10.5281/zenodo.18307401.

## VII. REFERENCES

[1] Gunasekar G, Krishnamurthy A, Thanarajan T, Rajendran S. SFoG-RPI: A Secured QoS Aware and Load Balancing Framework for FoG Computing in Healthcare Paradigm. Revue d'Intelligence Artificielle 2023;37:835–44. https://doi.org/10.18280/ria.370403.

[2] Thinakaran R, Suriayati S, Batumalay M. Motivation assessment model for intelligent tutoring system based on Mamdani inference system. IAES International Journal of Artificial Intelligence 2023;12:189–200. https://doi.org/10.11591/ijai.v12.i1.pp189-200.

[3] Kalbande D, Yuvaraj M, Verma MK, Subaveerapandiyan A, Suradkar P, Chavan S. Exploring the Integration of Artificial Intelligence in Academic Libraries: A Study on Librarians' Perspectives in India. Open Information Science 2024;8:Article 20240006. https://doi.org/10.1515/opis-2024-0006.

[4] Selvakumarasamy K, Nagabhooshanam N, Srividhya B, Valavan AT, Sivaraman R, Akhila BN, et al. EFFICIENT AI MODEL FOR RECOGNISING ABNORMAL NETWORKING ATTACKS IN CLOUD SYSTEM. Journal of Environmental Protection and Ecology 2024;25:1405–14.

[5] Zhou C, Jiang B. How do consumers react to AI-generated green marketing content? A hybrid analysis using PLS-SEM and text mining. Journal of Retailing and Consumer Services 2025;87:Article 104431. https://doi.org/10.1016/j.jretconser.2025.104431.

[6] Shlash Mohammad AA, Khanfar IAA, Al Oraini B, Vasudevan A, Mohammad SI, Fei Z. Predictive analytics on artificial intelligence in supply chain optimization | Análisis predictivo sobre inteligencia artificial en la optimización de la cadena de suministro. Data and Metadata 2024;3:Article 395. https://doi.org/10.56294/dm2024395.

[7] Sharma V, Payal R, Dutta K, Poulose J, Kapse M. A comprehensive examination of factors influencing intention to continue usage of health and fitness apps: a two-stage hybrid SEM-ML analysis. Cogent Business and Management 2024;11. https://doi.org/10.1080/23311975.2024.2391124.

[8] Xie X, Teng MF, Zhang LJ, Alamer A. Exploring AI Literacy and AI-Induced Emotions among Chinese University English Language Teachers: The Partial Least Square Structural Equation Modeling (PLS-SEM) Approach. International Journal of Applied Linguistics United Kingdom 2025;35:1897–911. https://doi.org/10.1111/ijal.12798.

[9] Karthikeyan M, Mahapatra DM, Razak ASA, Abahussain AAM, Ethiraj B, Singh L. Machine learning aided synthesis and screening of HER catalyst: Present developments and prospects. Catal Rev Sci Eng 2024;66:997–1027. https://doi.org/10.1080/01614940.2022.2103980.

[10] Li M, Noori AQ. Exploring the nexus of attitude, contextual factors, and AI utilization intentions: A PLS-SEM analysis among primary mathematics teachers in China. Asian Journal for Mathematics Education 2024;3:289–311. https://doi.org/10.1177/27527263241269060.

[11] Abbasi GA, Goh YN, Iranmanesh M, Liebana-Cabanillas F. Determinants of continuous intention to use retail apps: A hybrid PLS-ANN approach. Journal of Marketing Theory and Practice 2024;32:413–34. https://doi.org/10.1080/10696679.2023.2218098.

[12] Al-Emran M, Alqudah AA, Abbasi GA, Al-Sharafi MA, Iranmanesh M. Determinants of Using AI-Based Chatbots for Knowledge Sharing: Evidence From PLS-SEM and Fuzzy Sets (fsQCA). IEEE Trans Eng Manag 2024;71:4985–99. https://doi.org/10.1109/TEM.2023.3237789.

[13] Foudeh HAR, Yusoff Y, Zabil MHM, Cheng LK, Shariff MSM, Hafez MA. Statistical SEM-ANN Approaches for Metaverse Adoption in Education. J Stat Appl Probab 2025;14:667–81. https://doi.org/10.18576/jsap/140501.

[14] Alshahrani R, Yenugula M, Algethami H, Alharbi F, Shubhra Goswami S, Quadri Q, et al. Establishing the fuzzy integrated hybrid MCDM framework to identify the key barriers to implementing artificial intelligence-enabled sustainable cloud system in an IT industry. Expert Syst Appl 2024;238. https://doi.org/10.1016/j.eswa.2023.121732.

[15] Al-Sawaie KM, Abbas NA, AlSmeiran M, Alrawashdeh H, Vasudevan A, Yaseen H, et al. Estimating Potential Output Using a Production Function Approach. Applied Mathematics and Information Sciences 2025;19:271–8. https://doi.org/10.18576/amis/190204.

[16] He H, Bai S, Han C, Yang M, Fan W, Gupta BB. Beyond simple interaction: Uncovering the perception-interaction intrinsic mechanism of generative AI agents—A multi-modal big data analysis with PLS-SEM and fsQCA. Technol Soc 2025;83:Article 103020. https://doi.org/10.1016/j.techsoc.2025.103020.

[17] Popa RG, Popa IC, Ciocodeică DF, Mihălcescu H. Modeling AI Adoption in SMEs for Sustainable Innovation: A PLS-SEM Approach Integrating TAM, UTAUT2, and Contextual Drivers. Sustainability Switzerland 2025;17:Article 6901. https://doi.org/10.3390/su17156901.

[18] Bahçekapili E, Boztaş GD. Generative AI and digital literacy: Unravelling user intentions through PLS-SEM and machine learning. J Inf Sci 2025:Article undefined. https://doi.org/10.1177/01655515251396900.

[19] Qu C, Kim E. Investigating AI Adoption, Knowledge Absorptive Capacity, and Open Innovation in Chinese Apparel MSMEs: An Extended TAM-TOE Model with PLS-SEM Analysis. Sustainability Switzerland 2025;17:Article 1873. https://doi.org/10.3390/su17051873.

[20] Mohd Rahim NI, A. Iahad N, Yusof AF, A. Al-Sharafi M. AI-Based Chatbots Adoption Model for Higher-Education Institutions: A Hybrid PLS-SEM-Neural Network Modelling Approach. Sustainability Switzerland 2022;14:Article 12726. https://doi.org/10.3390/su141912726.

[21] Putthidech A, Bootwisas N, Intarasat U, Boonman P, Singchua W. The influence of AI-based learning perceptions on learning outcomes in calculus: The mediating role of cognitive and emotional responses using a PLS-SEM approach. Eurasia Journal of Mathematics Science and Technology Education 2025;21:Article em2738. https://doi.org/10.29333/ejmste/17390.

[22] Shahzad MF, Xu S, An X, Asif M, Javed I. Do generative AI technologies play a double-edged sword role in education? Findings from hybrid approach using PLS-SEM and fsQCA. Educ Inf Technol (Dordr) 2025;30:19647–76. https://doi.org/10.1007/s10639-025-13528-2.

[23] Rîndașu SM, Ionescu-Feleagă L, Ionescu B Ștefan, Topor SID. Digitalisation and Skills Adequacy as Determinants of Innovation for Sustainable Development in EU Countries: A PLS-SEM Approach | DIGITALIZAREA ȘI ADECVAREA COMPETENȚELOR CA FACTORI DETERMINANȚI AI INOVĂRII PENTRU DEZVOLTAREA DURABILĂ ÎN ȚĂRILE UE: O AB…. Amfiteatru Economic 2023;25:672–91. https://doi.org/10.24818/EA/2023/S17/968.

[24] López-Costa M, Donate-Beby B, Cabrera-Lanzo N, Maina MF. Understanding AI adoption among secondary education teachers: A pls-sem approach. Computers and Education Artificial Intelligence 2025;8:Article 100416. https://doi.org/10.1016/j.caeai.2025.100416.

[25] Terrah A, Abbasi GA, Ali F, Dogan S, Cobanoglu C. DETERMINANTS OF USERS' INTENTIONS TO USE AI-ENABLED TECHNOLOGICAL INNOVATIONS IN HOTELS: A HYBRID APPROACH USING PLS-SEM AND FSQCA. Advances in Hospitality and Tourism Research 2024;12:200–28. https://doi.org/10.30519/ahtr.1392494.